

Vibrational Analysis of Tangled Spectra. I. The Crystal Phase T←S Spectra of Acetophenone¹⁾

Kenichi NAKASHIMA[†] and Motohiko KOYANAGI*

Department of Chemistry, Faculty of Science, Kyushu University 33, Hakozaki Higashi-ku, Fukuoka 812

(Received May 7, 1984)

The T_{1,2}←S₀ phosphorescence excitation spectrum of acetophenone has been observed in a crystal at 4.2 K. The observed tangled vibronic structure is a manifestation that two states of different orbital types, ³ππ* and ³nπ*, lie close to each other. For the first time, the spectrum has been vibrationally analyzed in terms of the crude adiabatic Born-Oppenheimer vibronic states. The calculation is advanced *via* the following steps: (1) to assume appropriate zero-order vibronic level functions of both electronic excited states in the energy region 0–1000 cm⁻¹ above the T₁ phosphorescent origin level, (2) to take into account two different perturbations of vibronic and environmental interactions, (3) to establish a secular equation with two adjustable parameters for the evaluation of the off-diagonal matrix elements, (4) to diagonalize the equation after allocating appropriate values to the parameters, (5) to simulate the T←S spectrum, (6) to compare the simulation spectrum with the observed, (7) to revise several diagonal elements and the parameters if the comparison is not satisfied, and (8) to proceed with steps (1)–(7) until the simulation spectra accord with the observed. The results establish that the lowest excited triplet state of acetophenone in the crystal is ππ*, and that the next one is nπ* whose zero-order vibrationless level is postulated to lie at ≈400 cm⁻¹ higher than T₁⁰(0).

Aromatic carbonyls have been very attractive for molecular spectroscopists and photochemists because of the dynamical characteristics in the excited triplet states. There are reported many thereof,^{2–21)} and it has generally been accepted that the photochemical reactivity of such a molecule depends strongly upon whether its lowest triplet state is ππ* or nπ* and upon how large the energy separation is.^{22,23)} For the state assignments, of course, it is still valuable to vibrationally analyze the T→S emission and, especially, the T←S absorption spectra. Such T←S spectra, however, sometimes become very tangled, reflecting a heavy overlap of different electronic transition absorptions. As regards the tangled spectra of organic molecules, Wessel and McClure have done pioneering (and beautiful) work on the S_{1,2}←S₀ absorption spectra of naphthalene,²⁴⁾ and their work has been developed by several theoretical investigators.^{25–27)} Recently we have also been engaged in analyzing the tangled T←S spectra of benzaldehydes.^{28,29)}

Concerning the phosphorescent state of acetophenone in the crystal, there exists a serious discrepancy. On the basis of the intensity of the longest wavelength band (at 382.8 nm) and on the basis of an energy correlation between this and other related molecules, Dym and Hochstrasser concluded that the lowest excited triplet state is nπ*.³⁰⁾ From a study of the polarization and Zeeman effects on the origin band, Tanimoto *et al.* also came to the same conclusion³¹⁾ although they never rejected the alternative ππ* assignment which has been suggested from a study on dynamical properties of the triplet

state by Hirota *et al.*¹⁵⁾ From the polarization data, on the other hand, Case and Kearns assigned the longest wavelength band as ³L_a(ππ*)←S₀, and the 280 cm⁻¹ band as the origin of ³U(nπ*)←S₀,³²⁾ reversing the suggestion of Dym and Hochstrasser. A series of works on the zero field magnetic substates of acetophenone by Hirota *et al.* supported this assignment^{15,16)} although environments employed were different. On the basis of a study on the phosphorescence of 1% acetophenone in acetophenone-*phenyl-d*₅, Koyanagi *et al.* concluded that the phosphorescent state of crystal phase acetophenone is ππ*.⁷⁾ Recently, Souto and Lin have observed the phosphorescence spectra of acetophenone and its derivatives in *p*-dimethoxybenzene³³⁾ and suggested that the phosphorescent state is nπ*, preferring Dym and Hochstrasser's assignment³⁰⁾ to Case and Kearns'.³²⁾

The purpose of this paper is to analyze this tangled spectrum both experimentally and theoretically; and to give a clearcut answer to the controversial issue. The calculation method is based on making up secular equations with many crude BO vibronic state functions. The validity of the treatment will be manifested in comparison with the observed spectra.

Theoretical

The present treatment is, in principle, very simple and essentially the same as that reported elsewhere.^{28,29)} Here let us outline the major aspects and show a schematic block diagram of the calculation process (see Fig. 1).

We start with the assumptions that two excited electronic levels T₁⁰ and T₂⁰ lie close to each other and that there are vibronic and environmental interactions between them. For this system it is no longer

[†] Present address: Department of Food Science, Nishikyushu University, Kanzaki, Kanzaki-gun, Saga Prefecture 842.

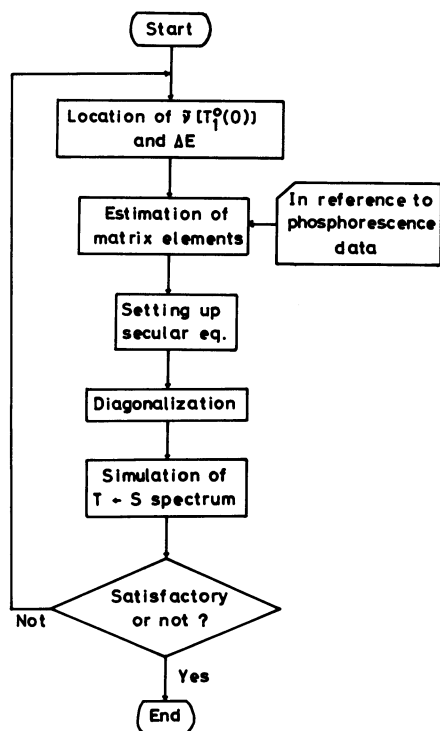


Fig. 1. Block diagram of the calculation process. ΔE is the energy separation between $T_1^0(0)$ and $T_2^0(0)$.

legitimate to use the general perturbation theory. The energies of the perturbed vibronic levels are then obtained by a direct diagonalization of the corresponding part of the energy matrix corrected to the first (or second) order, *i. e.*, by solution of the secular equation:

$$\begin{vmatrix} H_{11}-E & H_{12} & \cdots & H_{1m} & \cdots & H_{1n} \\ \cdot & H_{22}-E & \cdots & \cdot & \cdots & \cdot \\ \cdot & \cdots & \cdot & \cdots & \cdots & \cdot \\ H_{l1} & \cdots & \cdots & H_{ll}-E & H_{lm} & \cdots \\ \cdot & \cdots & \cdots & \cdot & \cdots & \cdot \\ H_{n1} & \cdots & \cdots & \cdots & \cdots & H_{nn}-E \end{vmatrix} = 0, \quad (1)$$

where

$$\begin{aligned} H_{lm} &= \langle l | H_0 + H' | m \rangle \\ &= \langle l | H_0 | m \rangle \delta_{lm} + \langle l | H' | m \rangle (1 - \delta_{lm}), \end{aligned} \quad (2)$$

and n is the number of vibronic levels considered. H_0 is the Hamiltonian of an idealized problem which can be solved exactly, while H' is the perturbation operator, *i. e.*, vibronic and environmental interactions.

$$H' = H_{\text{vib}} + H_{\text{environment}}. \quad (3)$$

Now, we need to evaluate the matrix elements of the coupling perturbation. If there is no vibronic level

degeneracy and the vibronic levels are described by a set of harmonic oscillator wavefunctions, it seems that the calculation is, in principle, straightforward. The zero-order eigenfunctions are given as the crude adiabatic wavefunctions of states T_1^0 and T_2^0 . Vibronic interactions, H_{vib} , are in general described as follows:³⁴⁾

$$\begin{aligned} H_{\text{vib}} &= \sum_a [\partial V(q, Q) / \partial Q_a]_0 Q_a \\ &\quad + 1/2 \sum_a \sum_b [\partial^2 V(q, Q) / \partial Q_a \partial Q_b]_0 Q_a Q_b + \cdots \\ &= H_{\text{vib}}(q, Q). \end{aligned} \quad (4)$$

Here Q_a and Q_b denote the a th and b th vibrational normal coordinates, respectively. On the other hand, $H_{\text{environment}}$ is given in the point-dipole approximation by³⁵⁾

$$\begin{aligned} H_{\text{environment}} &= - (e^2/R_{uv}^3) \sum_r \sum_{f,s} (2Z_r z_{f,s} - X_r x_{f,s} - Y_r y_{f,s}) \\ &\quad - (1/2) (e^2/R_{vv}^3) \sum_{f,s} \sum_{g,t} (2z_{f,s} z_{g,t} - x_{f,s} x_{g,t} - y_{f,s} y_{g,t}) \\ &= H_{\text{environment}}(q, Q; \xi_1, \xi_1; \xi_2, \xi_2; \cdots), \end{aligned} \quad (5)$$

where (X_r, Y_r, Z_r) denotes the coordinates of the r th electron of the solute molecule in question, $(x_{f,s}, y_{f,s}, z_{f,s})$ the coordinates of the s th electron of the f th environmental molecule.

For the evaluation of these two types of off-diagonal matrix elements in the acetophenone crystal, we prefer empirical methods to direct calculation. One of the methods is to find other suitable guest/host systems where the energy separation between T_1^0 and T_2^0 is very large. Optical data, if obtainable, will be useful for the evaluation of H_{lm} ($l \neq m$). If there is found no suitable guest/host system, another method is to utilize the spectral data of emissions which originate at the levels in "off-resonance region" and to take several practical assumptions. In the present work we employed this approach because of a failure in finding a suitable host system.

As shown in Eq. 5, $H_{\text{environment}}$ contains a number of solvent (environment) coordinates (ξ_f, ξ_f) together with the guest molecular coordinates (q, Q) . However, we treat this as an "averaged, static" perturbation on the "guest" molecule in question. In other words, we still consider the condensed phase problem in terms of the modulated electronic structure of the one guest molecule:

$$H_{\text{environment}} = H_{\text{environment}}(q, Q) \quad (6)$$

Similar treatments were reported elsewhere.^{35,36)} This type of perturbation may generally be taken into account for the spectra of molecules in

condensed media with poor site symmetry, and will allow the electrostatic couplings between intramolecular electronic states,^{35,37)} *e. g.*, direct couplings between T_1 and T_2 zero-point levels of aromatic carbonyls in rigid crystals as has been suggested by Hirota *et al.*¹⁵⁻¹⁷⁾ and Koyanagi *et al.*³⁸⁾

Several calculations were carried out for the following two cases: (1) $T_1=^3\pi\pi^*$ and $T_2=^3n\pi^*$; and (2) $T_1=^3n\pi^*$ and $T_2=^3\pi\pi^*$. Here, let us describe the detailed calculation method for case (1). Similar calculations are possible for case (2) (see the last subsection in "Results and Discussion"). For case (1) the secular determinant was made up using thirty-six crude adiabatic Born-Oppenheimer product functions, of which twenty-seven concern the $T_1(^3\pi\pi^*)$ electronic state and the others the $T_2(^3n\pi^*)$ state. For the $T_1(^3\pi\pi^*)$ state, we took into account eleven nontotally symmetric vibrations with low frequencies, *i. e.*, $\nu_{45}-\nu_{35}$; three phosphorescence-active totally symmetric vibrations, *i. e.*, ν_{30} , ν_{29} , ν_{27} , and their combination vibrations.³⁹⁾ The zero-order vibronic levels of $T_2(^3n\pi^*)$, are the vibrationless level, three in-plane vibrations (ν_{30} , ν_{29} , ν_{27}), and five low frequency out-of-plane vibrations ($\nu_{45}-\nu_{41}$). Several important vibrational modes are listed in Table 1.

Vibronic interaction matrix elements are given assuming Herzberg-Teller couplings.

$$\begin{aligned} & \langle T_1^0(0+\nu_i) | H_{vib} | T_2^0(0+\nu_j) \rangle_{(i \neq j)} \\ &= \langle ^3\pi\pi^* | \langle \partial V / \partial Q_i \rangle_0 | ^3n\pi^* \rangle \langle i_1 | Q_i | i_2 \rangle \langle j_1 | j_2 \rangle \prod_{k \neq i, j} \langle k_1 | k_2 \rangle \\ &+ \langle ^3\pi\pi^* | \langle \partial V / \partial Q_j \rangle_0 | ^3n\pi^* \rangle \langle j_1 | Q_j | j_2 \rangle \langle i_1 | i_2 \rangle \prod_{k \neq i, j} \langle k_1 | k_2 \rangle \\ &= \langle T_1^0(0+\nu_j) | H_{vib} | T_2^0(0+\nu_i) \rangle. \end{aligned} \quad (7)$$

Here $|T_1^0(0+\nu_i)\rangle$, for example, is the eigenstate function for the ν_i vibronic level of $T_1(^3\pi\pi^*)$ and $|k_2\rangle$ is that for the k -normal mode of $T_2(^3n\pi^*)$. The integrals, $\langle i_1 | Q_i | i_2 \rangle$ and $\langle j_1 | Q_j | j_2 \rangle$, yield a number of zero-valued matrix elements on the assumption of a set of harmonic oscillators. The overlap integrals, *e. g.*, $\langle i_1 | i_2 \rangle$ and $\langle j_1 | j_2 \rangle$, are related to the Franck-Condon factor in the transition $T_2 \leftarrow T_1$ (and that in the transition $T_2 \leftarrow S_0$ if the molecular structure is assumed to be identical both in the ground and first excited $^3\pi\pi^*$ state). The first order perturbation theory for a [weak vibronic coupling/large ΔE] system gives

$$\langle T_1^0(0+\nu_i) | H_{vib} | T_2^0(0) \rangle \propto I(i \leftarrow 0)^{1/2} \Delta E \propto I(0 \rightarrow i)^{1/2} \Delta E, \quad (8)$$

where ΔE is the energy separation between $T_1^0(0)$ and $T_2^0(0)$; $I(i \leftarrow 0)$ and $I(0 \rightarrow i)$ are the relative intensities of $T_1(0+\nu_i) \leftarrow S_0(0)$ absorption and $T_1(0) \rightarrow S_0(0+\nu_i)$ phosphorescence bands, respectively. Similarly,

$$\begin{aligned} & \langle T_1^0(0+\nu_i) | H_{vib} | T_2^0(0+\nu_j) \rangle_{(i_1 \neq a'', j_2 \neq a')} \\ & \propto I(i \leftarrow 0)^{1/2} \Delta E \langle 0_1 | j_2 \rangle \propto I(0 \rightarrow i)^{1/2} \Delta E \langle 0_1 | j_2 \rangle, \end{aligned} \quad (9)$$

TABLE 1. A PART OF ACETOPHENONE GROUND STATE VIBRATIONAL FREQUENCIES^{a)}

Mulliken numbering	Mode ^{b)}	$\tilde{\nu}/\text{cm}^{-1}$	Designation ^{c)}
<i>a''</i> species			
ν_{45}	COCH ₃ torsion	44	a
ν_{44}	CH ₃ torsion	125	b
ν_{43}	COCH ₃ wag	234	c
ν_{42}	ν_{16a}	421	d
ν_{41}	ν_{16b}	471	e
ν_{40}	ν_4	634	f
ν_{39}	ν_{10b}	692	g
ν_{38}	ν_{11}	768	h
ν_{37}	ν_{10a}	847	i
ν_{36}	ν_{17a}	945	j
<i>a'</i> species			
ν_{30}	δ (Ar-COCH ₃)	204	p
ν_{29}	δ (Ar-C-C)	376	q
ν_{27}	δ (C=O)	597	r
ν_8	ν (C=O)	1684	s

a) Taken from the reported crystal data (Ref. 7). b) The Wilson notation (Ref. 47). c) Band designations for Figs. 2, 4, and 5.

and so on.

Next let us write more practical assumptions. Two parameters were introduced for the evaluation of the off-diagonal matrix elements. They are f_v and F_e , where the former concerns the vibronic couplings and the latter the environmental couplings. These parameters were then refined in comparison with the simulated and observed spectra. Interaction matrix elements were evaluated from the relative intensity of the corresponding band of the $T_1 \rightarrow S_0$ phosphorescence spectrum⁷⁾ on the assumption of $\langle T_1^0(0) | H' | T_2^0(0+\nu_i) \rangle = \langle T_1^0(0+\nu_i) | H' | T_2^0(0) \rangle$ (see Eq. 7 for H_{vib} -terms); where H' is given by Eq. 3. The matrix elements $\langle T_1^0(0+\nu_i) | H_{vib} | T_2^0(0) \rangle$ were given as $f_v \times$ [the relative intensity of the corresponding vibronic band in the phosphorescence]^{1/2} (see Eqs. 8 and 9); the matrix elements $\langle T_1^0(0+\nu_i) | H_{environment} | T_2^0(0) \rangle$ were given as $F_e \times$ [Franck-Condon factor for the phosphorescence band $0 \rightarrow \nu_i$]^{1/2}. The parameter f_v is common to all the vibronic couplings and the successive quantity in brackets is uniquely determined from the phosphorescence intensity data. This leads to a considerable reduction from a tedious labor of fixing off-diagonal terms in a trial and error method. Similar simplification was carried out for $\langle T_1^0(0+\nu_i) | H_{environment} | T_2^0(0) \rangle$ by using the other parameter F_e .

All the $T \leftarrow S$ transition intensities were assumed to originate in zero-order transition $T_2^0(^3n\pi^*; 0,0)$ and three Franck-Condon vibronic transitions, $T_2^0(0,0+\nu_{30})$, $T_2^0(0,0+\nu_{29})$, and $T_2^0(0,0+\nu_{27})$, since there has, in general, been accepted the following relation for halogen-free aromatic carbonyls:^{8,41)}

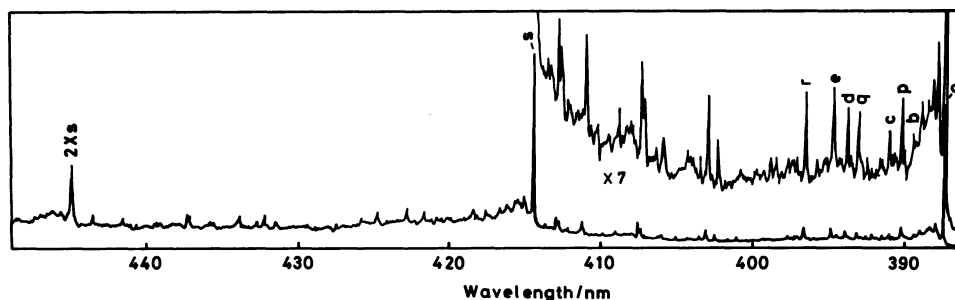


Fig. 2. Phosphorescence spectrum of $\approx 10^{-3}$ M acetophenone in *p*-dimethoxybenzene at 4.2 K. Band notations are defined in Table 1.

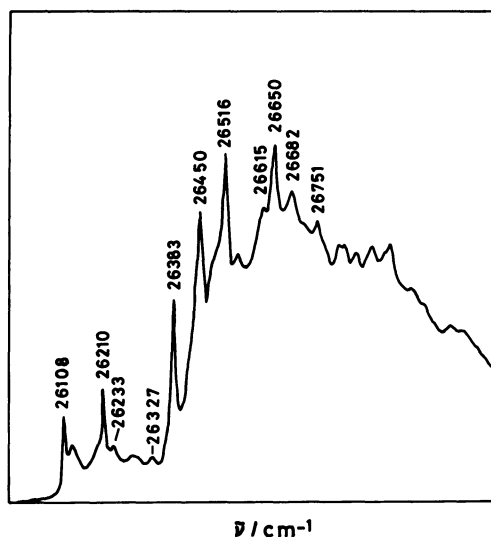


Fig. 3. $T_{1,2} \leftarrow S_0$ phosphorescence excitation spectrum of acetophenone in the crystal at 4.2 K.

$$f(^3n\pi^* \leftarrow S_0) \gg f(^3\pi\pi^* \leftarrow S_0). \quad (10)$$

Here $f(^3n\pi^* \leftarrow S_0)$ and $f(^3\pi\pi^* \leftarrow S_0)$ are the oscillator strengths of $^3n\pi^* \leftarrow S_0$ and $^3\pi\pi^* \leftarrow S_0$ transitions, respectively. The relative intensity ratios of $T_2^0(0,0)$, $T_2^0(0,0+\nu_{30})$, $T_2^0(0,0+\nu_{29})$, and $T_2^0(0,0+\nu_{27})$ were taken to be 1.000, 0.072, 0.051, and 0.086, respectively, as consulting the $T_1(n\pi^*) \rightarrow S_0$ phosphorescence spectrum of acetophenone in *p*-dimethoxybenzene at 4.2 K (Fig. 2).

For the evaluation of the diagonal matrix elements of $T_1^0(0+\nu_i)$, we started off with the same vibrational frequencies as those of the ground state (in other words, we assume almost the same molecular geometry of acetophenone in $^3\pi\pi^*$ as that in S_0),⁷ while somewhat different values for the diagonal matrix elements of $T_2^0(0+\nu_i)$ in reference to the $^1n\pi^* \leftarrow S_0$ transition vibrational data in *p*-dimethoxybenzene. The two parameters f_v and F_e were taken to be close to the values employed for the benzaldehyde T \leftarrow S spectra in acetophenone and methyl benzoate²⁸⁾

(*e.g.*, $f_v=55.0$ cm $^{-1}$ and $F_e=50.0$ cm $^{-1}$ for benzaldehyde in acetophenone).

Each absorption band was assumed to be of a lorentzian with a 10 cm $^{-1}$ full width at half maximum. Any interactions among intra- and intermolecular vibrations were ignored.

Experimental

Acetophenone (Aldrich and Wako Pure Chemical Co., Ltd.) was repeatedly distilled in vacuum. *p*-Dimethoxybenzene (Wako Pure Chemical Co., Ltd.) was purified by vacuum sublimation followed by zone-refining.

The T \leftarrow S phosphorescence excitation spectrum of acetophenone was observed using crystal samples in which a small amount of benzaldehyde was doped as an effective phosphorescence emitter. The $T_1 \rightarrow S_0$ phosphorescence and $S_1 \leftarrow S_0$ excitation spectra of acetophenone were also studied at 4.2 K in *p*-dimethoxybenzene single crystals which were prepared by the conventional Bridgman technique (the initial concentration of acetophenone: $\approx 10^{-3}$ M). All the spectra were recorded on a 3/4 m Nalumi Spectrophotometer. Other experimental details were similar to those described previously.⁴²⁾

Results and Discussion

Phosphorescence Spectrum of Acetophenone. The phosphorescence spectrum of acetophenone in *p*-dimethoxybenzene at 4.2 K is shown in Fig. 2. The phosphorescent state of acetophenone in *p*-dimethoxybenzene has been assigned to be $n\pi^*$ by Souto and Lin.³³⁾ We confirmed this. However, their vibrational assignment is considerably different from available normal-coordinate analysis data^{7,43)} and therefore seems to be erroneous especially for several out-of-plane vibrational modes. The present vibrational analysis is essentially based on the data by Koyanagi *et al.*⁷⁾ The results are shown in Fig. 2 together with alphabetical band designations whose vibrational notations are given in Table 1. Despite the propose $T_1=^3n\pi^*$ assignment,³³⁾ it is noticeable that there appear several out-of-plane vibrational bands which are weak, but discriminating (see bands *b*—*e* in Fig. 2).

T←*S* Spectrum of Acetophenone in the Crystal. The *T*←*S* excitation spectrum of acetophenone in the crystal is shown in Fig. 3. Sample crystals were prepared to contain $\approx 10^{-3}$ M benzaldehyde since the

TABLE 2. ZERO-ORDER DIAGONAL MATRIX ELEMENTS EMPLOYED^{a)}

Level	$\Delta\bar{\nu}/\text{cm}^{-1}$ b)	Level	$\Delta\bar{\nu}/\text{cm}^{-1}$ b)	Level	$\Delta\bar{\nu}/\text{cm}^{-1}$ b)
0>	0	27>	590	45*>	<u>50</u>
45>	70	40>	600	44*>	<u>125</u>
44>	90	39>	700	30*>	<u>170</u>
30>	190	38>	735	43*>	<u>195</u>
43>	245	37>	835	29*>	<u>360</u>
41>	325	36>	930	42*>	<u>380</u>
29>	360	35>	970	41*>	<u>430</u>
42>	445	0*>	<u>0</u>	27*>	<u>550</u>

a) For brevity we list only the fundamental vibronic levels. The asterisked states denote the BO vibronic levels of $T_1^0(n\pi^*)$ and the others $T_1^0(\pi\pi^*)$. b) Diagonal matrix elements are calculable on the basis: $|0>\leftrightarrow 26$ 150 cm^{-1} ; $|0*>\leftrightarrow 26$ 555 cm^{-1} . The underlined values give the energy separation from the $|0*>$ level.

dopant has been established to be an excellent triplet acceptor in the host.⁶⁾ The concentration ratios employed prove that the *T*←*S* absorption of the guest is weak enough on the present experimental conditions. Similarity of the *T*←*S* phosphorescence excitation spectrum (Fig. 3) to the direct *T*←*S* absorption spectrum (e. g., Fig.2 in Ref.31) assures this is the case.

The band at $26108\pm 2\text{ cm}^{-1}$ is taken to be the origin band of the $T_1\leftarrow S_0$ transition. This assignment is supported by the fact that the band location is in good agreement with the strong phosphorescence origin peak at $26100\pm 2\text{ cm}^{-1}$ which has been observed for the system of acetophenone in acetophenone-*phenyl-d*₅.⁷⁾ Almost all 20–60 cm^{-1} broad band features attending each prominent peak are assigned to be due to phonons. Main prominent bands are found at 26210, 26383, 26450, 26516, and 26650 cm^{-1} . The higher energy bands become the broader.

Simulated T←*S* Spectra of Acetophenone in the Crystal.

A diagonalization of the matrix was carried out and some parameters were refined. In Tables 2 and 3 we give the final estimates to zero-

TABLE 3. OFF-DIAGONAL MATRIX ELEMENTS EMPLOYED^{a)}

T_1^0	T_1^0								
	0*>	30*>	29*>	27*>	45*>	44*>	43*>	42*>	41*>
0>	70.00	18.55	17.50	56.42	33.24	55.34	30.68	85.00	41.56
30>	18.55	4.92	4.64	14.95	8.81	14.66	8.13	22.52	11.01
29>	17.50	4.64	4.37	14.10	8.31	13.83	7.67	21.25	10.39
27>	56.42	14.95	14.10	45.47	26.79	44.60	24.73	68.51	33.50
45>	33.24	8.81	8.31	26.79	0	0	0	0	0
44>	55.34	14.66	13.83	44.60	0	0	0	0	0
43>	30.68	8.13	7.67	24.73	0	0	0	0	0
42>	85.00	22.52	21.25	68.51	0	0	0	0	0
41>	41.56	11.01	10.39	33.50	0	0	0	0	0
40>	30.68	8.13	7.67	24.73	0	0	0	0	0
39>	17.00	4.50	4.25	13.70	0	0	0	0	0
38>	30.69	8.13	7.67	24.74	0	0	0	0	0
37>	21.67	5.74	5.42	17.47	0	0	0	0	0
36>	25.07	6.64	6.27	20.21	0	0	0	0	0
35>	25.07	6.64	6.27	20.21	0	0	0	0	0
45+30>	8.50	2.25	2.13	6.85	0	0	0	0	0
44+30>	13.86	3.67	3.46	11.17	0	0	0	0	0
43+30>	7.65	2.03	1.91	6.17	0	0	0	0	0
42+30>	21.25	5.63	5.31	17.13	0	0	0	0	0
41+30>	10.37	2.75	2.59	8.36	0	0	0	0	0
45+29>	8.50	2.25	2.13	6.85	0	0	0	0	0
44+29>	13.60	3.60	3.40	10.96	0	0	0	0	0
43+29>	7.65	2.03	1.91	6.17	0	0	0	0	0
42+29>	21.25	5.63	5.31	17.13	0	0	0	0	0
41+29>	10.37	2.75	2.59	8.36	0	0	0	0	0
45+27>	8.50	2.25	2.13	6.85	0	0	0	0	0
44+27>	13.60	3.60	3.40	10.96	9	0	0	0	0

a) In cm^{-1} units.

order energies and interaction values on the assumption of $T_1=3\pi\pi^*$.⁴⁴⁾ Figure 4(a) shows the location of zero-order levels; and the height of the solid lines represents the relative interaction energies between $T_1^0(0+\nu_i)$ and $T_2^0(0)$ and the height of dashed lines the

interactions between $T_1^0(0)$ and $T_2^0(0+\nu_i)$. The longest wavelength band at 26108 cm^{-1} in the simulated T←S spectrum is assigned to the origin band of the $T_1(\pi\pi^*)\leftarrow S_0$ transition as is confirmed by analyzing the eigenvectors given in Table 4. The corresponding state is described by a large component of $|T_1^0(0)\rangle$ and a small part of other zero-order vibronic eigenvectors:

$$\begin{aligned} \psi_{T_1(0)} \simeq & -0.95|0\rangle + 0.20|0^*\rangle \\ & -0.12|44\rangle + 0.10|42^*\rangle, \end{aligned} \quad (11)$$

where $|0\rangle$ and $|0^*\rangle$ represent $|T_1^0(0)\rangle$ and $|T_2^0(0)\rangle$, respectively. There is found considerable $|0^*\rangle$ mixing with $|0\rangle$. This will explain why the origin band of the $T_1\leftarrow S_0$ absorption appears with remarkable intensity despite the proposed $\pi\pi^*$ assignment. The major part of the state function, however, is zero-order function $|0\rangle$. This means that many physical properties for this state are still under the control of the zero-order function $|0\rangle$ except for several optical properties such as the absorption band intensity, polarization, and emission lifetime. The -0.12 value of the expansion coefficient for $|44\rangle$ seems to be due to the second-order coupling through $|0^*\rangle$ as an intermediate level.

The observed bands at 26210 cm^{-1} and 26233 cm^{-1} are assigned as $T_1(0,0+\nu_{45})$ and $T_1(0,0+\nu_{44})$, respectively, since their corresponding state functions contain a large coefficient of either $|45\rangle$ or $|44\rangle$. It should, however, be noted that a considerable mixing of the other zero-order function is also found (see Table 4). These mixings possibly occur *via* second-order vibronic couplings with an intermediate state, $|0^*\rangle$, if the relevant levels (ν_{45} and ν_{44}) are lying close to each other. It is, thus, not surprising to see that the band $T_1(0,0+\nu_{45})$ is more intense than $T_1(0,0+\nu_{44})$ despite of the reverse magnitude relation of the employed interaction matrix elements, *i.e.*, $|\langle 45|H'$

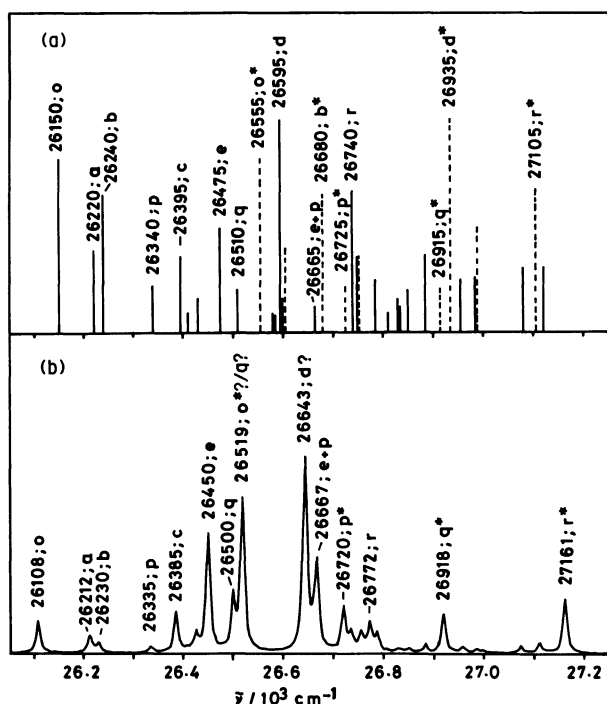


Fig. 4. (a) The zero-order vibronic levels of $T_1^0(\pi\pi^*)$ and $T_2^0(n\pi^*)$. The solid and dashed lines show the zero-order T_1^0 and T_2^0 vibronic levels, respectively. The length of each line shows the relative value of the off-diagonal matrix element between the relevant vibronic level and the zero-order vibrationless level of the counterpart electronic state. (b) Simulated $T_{1,2}\leftarrow S_0$ transition spectrum of acetophenone in the crystal. The bands are assumed to be a Lorentzian, each band having a 10 cm^{-1} width.

TABLE 4. VIBRONIC EIGENFUNCTIONS FOR REPRESENTATIVE BANDS OF ACETOPHENONE IN THE CRYSTAL^{a)}

BO basis function	State ^{b)}							
	26108 (26108)	26212 (26210)	26230 (26233)	26335 (26327)	26385 (26383)	26450 (26450)	26519 (26516)	26643 (26650)
$ 0\rangle$	-0.946	-0.159	-0.100	-0.073	0.071	-0.097	0.063	0.086
$ 45\rangle$	-0.081	0.892	-0.427	-0.029	0.053	-0.062	0.050	0.029
$ 44\rangle$	-0.115	0.386	0.889	-0.060	0.101	-0.113	0.089	0.051
$ 30\rangle$	-0.045	0.021	0.021	0.986	0.096	-0.070	0.035	0.037
$ 43\rangle$	-0.029	0.032	0.027	0.056	-0.934	-0.233	0.110	0.046
$ 41\rangle$	-0.031	0.030	0.025	0.031	-0.125	0.766	0.413	0.091
$ 29\rangle$	-0.024	0.008	0.007	0.020	-0.034	0.127	0.554	0.079
$ 42\rangle$	-0.047	0.042	0.034	0.034	-0.108	0.256	-0.516	0.643
$ 0^*\rangle$	0.197	-0.143	-0.110	-0.083	0.220	-0.377	0.428	0.480
$ 42^*\rangle$	0.103	0.016	0.010	-0.031	-0.009	0.003	-0.029	0.050

a) Here the expansion coefficients are shown for only the major BO functions. b) The state functions are denoted by the band energies (eigenvalues). The values in parentheses are the observed data.

$|0^*\rangle \langle 44|H'|0^*\rangle$. Similarly, from the coefficient analysis, the band at 26327 cm^{-1} is attributed to $T_1(0,0+\nu_{30})$.

Next, let us view the band-crowded region which starts on the lower energy tail of the 26383 cm^{-1} band (Fig. 3). At a glance, there are four prominent bands superimposed on the broadened background: the bands at 26383 , 26450 , 26516 , and 26650 cm^{-1} . Their corresponding state functions are approximately expressed as follows:

$$|26383\rangle \simeq 0.22|0^*\rangle - 0.93|43\rangle - 0.11|42\rangle - 0.13|41\rangle \quad (12)$$

$$|26450\rangle \simeq -0.38|0^*\rangle - 0.23|43\rangle + 0.26|42\rangle + 0.77|41\rangle \quad (13)$$

$$|26516\rangle \simeq 0.43|0^*\rangle + 0.55|29\rangle - 0.52|42\rangle + 0.41|41\rangle \quad (14)$$

$$|26650\rangle \simeq 0.48|0^*\rangle - 0.36|27\rangle + 0.64|42\rangle + 0.26|44^*\rangle. \quad (15)$$

A large mix-up in these state functions is noticeable. The states corresponding to the bands at 26383 and 26450 cm^{-1} have components large enough so that they can safely be attributed to $T_1(0,0+\nu_{43})$ and $T_1(0,0+\nu_{41})$, respectively. However, the other two states do not meet our criterion²⁸⁾ for unique assignment.⁴⁶⁾

As shown clearly in Table 4, the vibronic state functions are canonically described by a number of crude adiabatic BO state functions and there is considerable environmental mixing between $T_1^0(\pi\pi^*)$ and $T_2^0(n\pi^*)$. The environmental mixing is more prominent in this acetophenone case than in benzaldehyde case,²⁸⁾ as is rationalized by the easily detectable origin band (see band at 26108 cm^{-1} in Fig.

3).

We previously gave a CNDO description of $^3n\pi^*$ and $^3\pi\pi^*$ states for benzaldehyde.²⁸⁾ Similar consideration for acetophenone predicts: (i) the π and π^* orbitals are strongly bonding and antibonding in the C=O region, respectively; (ii) the expectable change in acetyl group bond order brought about by $\pi^* \leftarrow n$ promotion leads to a large reduction in C=O stretching vibrational frequency and a small reduction in C-CH₃ vibrational frequency on going from the ground state to the $n\pi^*$ excited state; and (iii) the large increase in the C-COCH₃ bond order is realized consequent to $\pi^* \leftarrow \pi$ promotion, while its small increase on $\pi^* \leftarrow n$ promotion. The prediction (iii) leads us to expect ν_{45} and ν_{43} frequencies increase on going from the ground to the excited states. In Table 5 are summarized several vibrational data employed for the three electronic states. Although ν_{42} essentially belongs to the ring modes, an introduction of a methyl group to the C=O group has been known to bring forth a large mode-mixing between $\omega(\text{CXO})$ and so-called Wilson's ν_{16a} modes.^{7,47)} The mode frequency increase in ν_{43} and ν_{42} , thus, seems to be rationalized to a certain extent. Another notable point in Table 5 is that ν_{41} mode drastically decreases in frequency on going from S_0 to T_1 . For the present we cannot explain this.

As regards off-diagonal matrix elements, the values given previously for benzaldehyde²⁸⁾ are good references. For convenience sake, let us take and compare two representative off-diagonal terms with large values. The prominent values of $\langle T_1^0|H_{\text{environment}}|T_2^0\rangle$ are 36.0 , 50.0 , and 70.0 cm^{-1} for benzaldehyde/methyl benzoate, benzaldehyde/acetophenone, and acetophenone crystal, respectively, while the largest vibronic interaction matrix elements are 67.5 cm^{-1} (for H-wag), 55.0 cm^{-1} (for H-wag), and 85.0 cm^{-1} (for ν_{42}).

Simulation Spectra for the Reverse Case to the $T_1=^3n\pi^$ Assignment* loc. cit.

We carried out a series of calculations on the assumption that the lowest excited triplet state of crystal phase acetophenone is of $\pi\pi^*$. Good agreement between the observed and simulated spectra seems to establish our assignment. It is, however, necessary to refer to the results of calculations which we carried out under the reverse assignment, i.e., $T_1=^3n\pi^*$ and $T_2=^3\pi\pi^*$. Figure 5 shows the simulation spectrum where only the two zero-order energies are changed into: $E[T_1^0(n\pi^*;0,0)]=26150\text{ cm}^{-1}$ and $E[T_2^0(\pi\pi^*;0,0)]=26555\text{ cm}^{-1}$; and where all the other parameters are the same as those loc. cit.⁴⁸⁾ It should be noted that "the spectrum is characterized by the extremely intense T_1 origin band and very weak out-of-plane vibrational bands." This character is, more or less, kept for many other ΔE values except for $|\Delta E| < 50\text{ cm}^{-1}$ where the crystal field couplings between the

TABLE 5. VIBRATIONAL FREQUENCIES PROPOSED FOR SEVERAL IMPORTANT MODES OF ACETOPHENONE IN THE EXCITED TRIPLET STATES^{a)}

Vibration	Frequency		
	S_0	T_1	T_2
ν_{45}	44	70	50
ν_{44}	125	90	125
ν_{43}	234	245	195
ν_{42}	421	445	380
ν_{41}	471	325	430
ν_{30}	204	190	170
ν_{27}	597	590	550

a) In cm^{-1} units. For comparison, the ground state frequencies taken from the observed values (Ref. 7) were given in the second column. The other frequency values cited were taken on the basis of the present calculation.

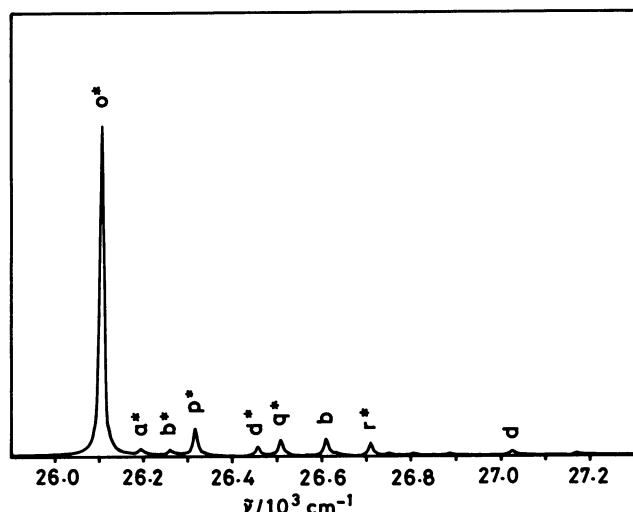


Fig. 5. Hypothetical T \leftarrow S spectrum of acetophenone. Here $T_1^0 = {}^3n\pi^*$ and $T_2^0 = {}^3\pi\pi^*$ were assumed. $\Delta E = 405 \text{ cm}^{-1}$.

zero-order vibrationless levels are considerable so that there appears generally a "doublet" band structure.⁵⁰ Similar " $n\pi^*$ " type band patterns have also been demonstrated for benzaldehyde T \leftarrow S spectra in methylcyclohexane.^{29, 42} In conclusion we do not believe that T_1 is $n\pi^*$ in crystalline acetophenone.

Concluding Remarks

Two different assignments for the lowest excited triplet state of acetophenone in the crystal have been proposed.^{5, 7, 30-32} The present treatment shows that T_1 is $\pi\pi^*$. Almost all observed T \leftarrow S bands are assignable as $T_1(\pi\pi^*)$ vibronic bands which are strongly coupled with $T_2(n\pi^*)$ origin band.

Many investigators have so far searched for the $n\pi^*-\pi\pi^*$ criterion "measures" by which the lowest excited triplet state is discernible: e.g., radiative lifetimes, deuteration shifts, zero-field splittings, spectral band patterns, Zeeman effects, Stark effects, etc. (for these problems, see Ref. 54). It seems, however, that there are no decisive "measures" for the criterion. We believe the present treatment could throw a light on the long-time controversial issues.

Lastly, we would like to mention phonons. We have not explicitly taken into account the role of phonon modes in the present theoretical treatment. There remains the problem of deciding whether we should take into account phonons as vibronic coupling modes or Franck-Condon modes. We will refer to this problem in the following paper.⁴⁵

The authors acknowledge helpful discussions with Professor Donald S. McClure (Princeton University) and Professor Lionel Goodman (Rutgers University) at the earliest stage of this work on the vibronic

interactions of congested electronic systems, and invaluable suggestions by referees. One of the authors (KN) wishes to express thanks to Professor R. Shimada for his warm hospitality and encouragements in Kyushu University. The calculations reported in this paper have been carried out at the Computation Center of Kyushu University.

References

- 1) A preliminary report of this work was presented at the National Symposium on Molecular Structure and Molecular Spectroscopy, Aug. 31-Sept. 3, 1983, Sendai, Japan.
- 2) Y. Kanda, H. Kaseda, and T. Matsumura, *Spectrochim. Acta*, **20**, 1387 (1964).
- 3) R. Shimada and L. Goodman, *J. Chem. Phys.*, **43**, 2027 (1965).
- 4) T. Takemura and H. Baba, *Bull. Chem. Soc. Jpn.*, **42**, 2756 (1969).
- 5) Y. H. Li and E. C. Lim, *Chem. Phys. Lett.*, **7**, 15 (1970).
- 6) M. Koyanagi and L. Goodman, *J. Chem. Phys.*, **55**, 2959 (1971).
- 7) M. Koyanagi, R. J. Zwarich, and L. Goodman, *J. Chem. Phys.*, **56**, 3044 (1972).
- 8) L. Goodman and M. Koyanagi, *Mol. Photochem.*, **4**, 369 (1972).
- 9) M. Koyanagi and L. Goodman, *Chem. Phys.*, **39**, 237 (1979).
- 10) H. Hayashi and S. Nagakura, *Mol. Phys.*, **24**, 801 (1972).
- 11) H. Hayashi and S. Nagakura, *Chem. Phys. Lett.*, **18**, 63 (1973).
- 12) H. Hayashi and S. Nagakura, *Mol. Phys.*, **27**, 969 (1974).
- 13) T. H. Cheng and N. Hirota, *Chem. Phys. Lett.*, **13**, 194 (1972).
- 14) T. H. Cheng and N. Hirota, *J. Chem. Phys.*, **56**, 5019 (1972).
- 15) T. H. Cheng and N. Hirota, *Mol. Phys.*, **27**, 281 (1974) and references cited therein.
- 16) S. W. Mao and N. Hirota, *Mol. Phys.*, **27**, 309 (1974).
- 17) E. T. Harrigan and N. Hirota, *Mol. Phys.*, **31**, 681 (1976).
- 18) Y. Hirata and N. Hirota, *Mol. Phys.*, **39**, 129 (1980).
- 19) E. Migirdicyan, *J. Chem. Phys.*, **55**, 1861 (1971).
- 20) A. Despres, V. Lejeune, and E. Migirdicyan, *Chem. Phys.*, **36**, 41 (1979).
- 21) A. Despres, V. Lejeune, and E. Migirdicyan, *Chem. Phys.*, **66**, 57 (1982).
- 22) P. Wagner, A. E. Kemppainen, and H. N. Schott, *J. Am. Chem. Soc.*, **92**, 5280 (1970).
- 23) P. Wagner, A. E. Kemppainen, and H. N. Schott, *J. Am. Chem. Soc.*, **95**, 5604 (1973).
- 24) J. Wessel, Ph. D. Thesis, University of Chicago, Chicago, 1971; J. Wessel and D. S. McClure, *Mol. Cryst. Liq. Cryst.*, **58**, 121 (1980).
- 25) C. A. Langhoff and G. W. Robinson, *Chem. Phys.*, **6**, 34 (1974).
- 26) H. K. Hong, *Chem. Phys.*, **9**, 1 (1975).
- 27) J. O. Berg, *Chem. Phys. Lett.*, **41**, 547 (1976).
- 28) M. Koyanagi, K. Nakashima, and L. Goodman,

Chem. Phys., **92**, 435 (1985). See also Ref. 24 for the theoretical backgrounds of the analysis of tangled spectra.

29) M. Koyanagi and K. Nakashima, *Chem. Phys.*, **90**, 399 (1984).

30) S. Dym and R. M. Hochstrasser, *J. Chem. Phys.*, **51**, 2458 (1969).

31) Y. Tanimoto, T. Azumi, and S. Nagakura, *Bull. Chem. Soc. Jpn.*, **48**, 136 (1975).

32) W. A. Case and D. R. Kearns, *J. Chem. Phys.*, **52**, 2175 (1970). Recently somewhat different polarization data were reported by Tanimoto *et al.* (Ref. 31).

33) M. A. Souto and C. T. Lin, *Chem. Phys.*, **17**, 129 (1976).

34) T. Azumi and K. Matsuzaki, *Photochem. Photobiol.*, **25**, 315 (1977) and references cited therein.

35) M. Koyanagi, *J. Mol. Spectrosc.*, **25**, 273 (1968).

36) G. W. Robinson, *J. Mol. Spectrosc.*, **6**, 58 (1961).

37) G. W. Robinson, *J. Chem. Phys.*, **46**, 572 (1967).

38) M. Koyanagi, K. Higashi, and Y. Kanda, *Chem. Phys. Lett.*, **52**, 184 (1977).

39) Here we employed Mulliken mode numbering (Ref. 40). See also Table I for Wilson notations which have been employed in Refs. 7 and 33.

40) R. S. Mulliken, *J. Chem. Phys.*, **23**, 1997 (1955).

41) S. P. McGlynn, T. Azumi, and M. Kinoshita, "Molecular Spectroscopy of the Triplet State," Prentice-Hall, Englewood Cliffs, New Jersey (1969), Chap. 6.

42) L. Goodman, M. Lamotte, and M. Koyanagi, *Chem. Phys.*, **47**, 329 (1980).

43) A. Gambi, S. Giorgianni, A. Passerini, R. Visinoni, and S. Gheretti, *Spectrochim. Acta*, **36A**, 871 (1980).

44) To simplify the calculation, here we neglected the following type matrix elements: $\langle T_1^0(0+\nu_i) | H_{\text{environment}} | T_2^0(0+\nu_i) \rangle$, where ν_i is an out-of-plane vibrational mode. This integral, in general, leads to minor mixing between the relevant vibronic levels. The magnitude of such mixing, in many cases, is close to that of the mixing between $T_1^0(0)$ and $T_2^0(0)$. This point will be discussed in the succeeding paper (Ref. 45).

45) K. Nakashima and M. Koyanagi, *Bull. Chem. Soc. Jpn.*, the succeeding paper.

46) It is tempting to accept a suggestion that these bands are attributed to $T_1(0,0+\nu_{29})$ and $T_1(0,0+\nu_{42})$, respectively, from the component analysis. For the former, however, we have an explicit calculation band at 26500 cm^{-1} whose state function is expressed as follows:

$$|26500\rangle \simeq 0.25|0^*\rangle - 0.80|29\rangle \\ - 0.25|42\rangle + 0.43|41\rangle.$$

47) E. B. Wilson, J. C. Decius, and P. C. Cross, "Molecular Vibration" McGraw Hill, New York (1955).

48) As for off-diagonal vibronic interaction matrix elements, we employed the same values as in case (1) where $T_1=^3\pi\pi^*$ was assumed. Even if the phosphorescence spectrum of acetophenone in acetophenone-*phenyl-d*₅ is of $n\pi^*$ nature, no big change for the vibronic interaction matrix elements $\langle ^3n\pi^* | H_{\text{vib}} | ^3\pi\pi^* \rangle$ will be necessary because the phosphorescence band pattern of acetophenone in acetophenone-*phenyl-d*₅ is considerably similar to that in benzoic acid reported by Nagaoka and Hirota (Ref. 49). Without doubt the phosphorescence in benzoic acid host is of $\pi\pi^*$.

49) S. Nagaoka and N. Hirota, *Bull. Chem. Soc. Jpn.*, **56**, 3381 (1983).

50) Here we completely neglected spin-orbit couplings between $^3n\pi^*$ and $^3\pi\pi^*$. This seems to be rationalized to a great extent as long as we are concerned with optical spectra in the case of $|\Delta E| > 50 \text{ cm}^{-1}$. For $|\Delta E| < 50 \text{ cm}^{-1}$, large (8–15 cm^{-1}) spin-sublevel splitting spectra have been observed because of considerable spin-orbit couplings (see Refs. 51–53).

51) H. J. Griesser and R. Bramley, *Chem. Phys.*, **67**, 361, 373, (1982).

52) M. R. Taherian and A. H. Maki, *Chem. Phys.*, **68**, 179 (1982).

53) M. Koyanagi, T. Terada, and Y. Kanda, *J. Chem. Phys.*, to be published.

54) K. Nakashima and M. Koyanagi, *Chem. Phys. Lett.*, **110**, 85 (1984).